Ecological Indicators 67 (2016) 227–237

Contents lists available at ScienceDirect

Ecological Indicators

journal homepage: www.elsevier.com/locate/ecolind

Is *Tillandsia capillaris* an efficient bioindicator of atmospheric metal and metalloid deposition? Insights from five months of monitoring in an urban mining area

Eva Schreck[a], Géraldine Sarret[b], Priscia Oliva[a], Aude Calas[a,i], Sophie Sobanska[c], Stéphane Guédron[b], Fiorella Barraza[a], David Point[a], Carlos Huayta[d], Raoul-Marie Couture[e,f], Jonathan Prunier[a], Manuel Henry[a], Delphine Tisserand[b], Sylvaine Goix[a,g], Jaime Chincheros[h], Gaëlle Uzu[i,j,*]

[a] *Géosciences Environnement Toulouse (GET), Observatoire Midi Pyrénées, Université de Toulouse CNRS, IRD, 14 avenue E. Belin, F-31400 Toulouse, France*
[b] *ISTerre, UMR 5275, Université Grenoble Alpes, CNRS, F-38041 Grenoble, France*
[c] *LASIR (UMR CNRS 8516), Université de Lille 1, Bât. C5, 59655 Villeneuve d'Ascq Cedex, France*
[d] *Government of Oruro, Environmental Department, Bolivia*
[e] *Norwegian Institute for Water Research – NIVA, NO-0349 Oslo, Norway*
[f] *Earth and Environmental Sciences Department, University of Waterloo, Waterloo, Ontario N2L 3G1, Canada*
[g] *Institut Ecocitoyen, Centre de vie la Fossette RD 268, 13270 Fos-sur-Mer, France*
[h] *Laboratorio de calidad ambiental, Universidad Mayor de San Andrés, Cota cota, La Paz, Bolivia*
[i] *Université Grenoble Alpes, LTHE, F-38000 Grenoble, France*
[j] *IRD, LTHE, F-38000 Grenoble, France*

ARTICLE INFO

Article history:
Received 16 October 2015
Received in revised form 18 January 2016
Accepted 7 February 2016
Available online 25 April 2016

Keywords:
Tillandsia capillaris
Passive filters
Air quality
Biomonitoring
Mining area

ABSTRACT

Atmospheric pollution in megacities has a major impact on human health and environmental quality. Air quality bioindicators may have some advantages over standard devices such as impactors or filters. In this study we evaluated the reliability of *Tillandsia* sp. *versus* passive filters for monitoring the atmospheric deposition of metal(loid)s in an area affected by anthropogenic activities. We aimed to gain insight into the composition and origin of atmospheric particles and their fate after deposition on the plant. Three zones with different contamination levels were monitored for five months in 2012. For the highly contaminated area, a linear increase in metal(loïd) accumulation was found in passive filters, whereas for transplanted *Tillandsia capillaris* the increase was almost linear for As, Cd, Hg, and Sn, but not for Ag, Pb, Sb, and Zn. For the moderately contaminated zone, the results showed that the exposure time was not sufficient for metal(loid) concentrations to increase in either the plants or filters. However, natural specimens provided some indications of the levels of metal contamination. Metal particles were observed on the plant surface and also in the central disc underneath tillandsia trichomes, suggesting that this is a possible pathway for metals to enter the plant. X-ray absorption spectroscopy demonstrated chemical transformation for Pb and As, both in filters and plants. For Pb, sorbed Pb and/or cell wall complexes were identified in the plants. No As^{III}-S species, indicative of As detoxification, were identified in the plant. Arsenic was oxidized from As^{III} to As^{V} in both plants and filters. Thus, in the present study, passive filters proved more reliable than *T. capillaris* transplants, although natural specimens provided some insights into local contamination. Particulate contaminants underwent chemical transformation after being trapped in the plant, but there was no clear evidence of internalization and detoxification.

1. Introduction

Atmospheric pollution in megacities is becoming a crucial environmental and health issue (Gao et al., 2011; OíNeill et al., 2013; Qian et al., 2014; Timmermans et al., 2013; Vanos et al., 2014). In emerging Latin America countries, sources of contamination in rapidly growing cities include industrial and mining activities, as well as traffic (Romero-Lankao et al., 2013). Beside new regulations on emissions, air pollution monitoring is increasingly needed. In many areas in the world, standard techniques for air monitoring are prohibitive in terms of cost. Biomonitoring methods using mosses, lichens and epiphytic bromeliads (*i.e.*, *Tillandsia*) have thus

* Corresponding author. Tel.: +33 456520994.
E-mail address: gaelle.uzu@ird.fr (G. Uzu).

http://dx.doi.org/10.1016/j.ecolind.2016.02.027
1470-160X/

been suggested as low cost alternatives (Ares et al., 2012; Bermudez et al., 2009; Szczepaniak and Biziuk, 2003; Grangeon et al., 2012). Biomonitoring can be done by collecting natural specimens, or by exposing transplanted specimens for a given duration. The latter option may provide more precise monitoring after validation and calibration with other types of air monitors.

Several species of *Tillandsias* were tested as biomonitors of metals and metalloids, volatile organic compounds and polycyclic aromatic hydrocarbons. Most of these studies were conducted in Latin America due to the widespread distribution of these plants, their resistance to high hydric stress and desiccation (Bermudez et al., 2009; Abril et al., 2014; Carreras et al., 2009; Figueiredo et al., 2007; Isaac-Olivé et al., 2012; Martínez-Carrillo et al., 2010). *Tillandsia* spp. use their epidermal trichomes to absorb atmospheric water, minerals and organic nutrients (Martin et al., 2013). The trichomes have a shield-like shape, formed by an axis (stem) connected to the internal tissues, and by an external shield. Trapped water and nutrients go through the shield cells, stem, and finally reach the underlying mesophyll parenchyma along a symplasmic route (Papini et al., 2010).

Several studies showed some correspondence between atmospheric emissions or human activities and metal accumulation in *Tillandsia capillaris* (Bermudez et al., 2009; Abril et al., 2014; Wannaz et al., 2006; Goix et al., 2013) and *T. usneoides* (Martínez-Carrillo et al., 2010). However, metal retention capacities and accumulation kinetics varied among studies, species and chemical elements. Some studies reported that plants reached maximal metal loads after a certain exposure time, ranging from a few weeks to a few months (Martínez-Carrillo et al., 2010 and refs therein). A decrease in metal content was observed in other cases (Bermudez et al., 2009; Abril et al., 2014; Wannaz et al., 2006; Bermudez and Pignata, 2011). In highly polluted areas, toxicity symptoms were observed (Bermudez et al., 2009; Wannaz et al., 2006, 2011, 2012), which may have potentially affected metal accumulation. The fate of particles deposited on the plant surface including possible chemical transformation, transfer to internal parts of the plant, and excretion, may affect accumulation and the efficiency of the plant as a biomonitor. Very little is known on these aspects, except for Cs (Li et al., 2012) and Hg (Amado Filho et al., 2002).

The aims of the present study were to: (i) evaluate the reliability of *T. capillaris versus* passive filters for airborne metal(loid)s contamination monitoring in an area impacted by mining, smelting and urban activities, (ii) study the influence of the seasonality on metal(loid) accumulation, and (iii) gain insights on the fate of trapped particles inside the plant. Samples were characterized using a combination of chemical analyses, scanning transmission microscopy coupled with energy dispersive spectrometry (SEM-EDX), and X-ray absorption spectroscopy. For the latter technique, As and Pb were chosen as target elements. Both are relevant for safety issues and pathologies around the world (Jarup, 2003) and specifically in this area of Oruro, the major mining city in Bolivia (Fontúrbel et al., 2011). Lead is a ubiquitous atmospheric contaminant, and the foliar uptake of Pb-rich particles was studied recently (Schreck et al., 2014; Uzu et al., 2010; Uzu et al., 2014). Atmospheric As contamination has been much less studied. However, in Oruro, As concentrations reached 200 ng m^{-3} (Goix et al., 2011), which is significantly above the regulation threshold of 5 ng m^{-3}. In the environment, As exists predominantly in the +3 and +5 oxidation states, present as arsenite (AsO_3^{3-}) and arsenate (AsO_4^{3-}) oxyanions in aqueous solution, respectively. In contrast, Pb occurs as a divalent cation in the environment and, to a lesser extent, as elemental Pb in highly contaminated areas. From these different chemical reactivities, different chemical transformations in the atmosphere, bioaccumulation and transformation in the plant may be expected.

This study was conducted in 2012 in Oruro (Bolivia) where air, soil, plants and urban dust are significantly contaminated by a mixture of metal(loid)s due to mining (polymetallic sulfides) and Sn smelting activities (Goix et al., 2013; Fontúrbel et al., 2011; Goix et al., 2011; Ruiz-Castell et al., 2012; Van Damme et al., 2010; Miller and Villarroel, 2011; Terán-Mita et al., 2013). Urban activities such as residential and municipal combustion of fossil fuel and automotive traffic also contribute. The kinetics of metal and metalloid accumulation in *T. capillaris* and in passive filters exposed for five months to various sources of contamination (mining, smelting and urban activities) was studied. Elemental concentrations were compared to natural specimens exposed to contaminants for several years in the same area. The localization and speciation of the contaminants trapped in transplanted and natural plants and in the filters were compared.

2. Materials and methods

2.1. Biological material and preparation of plants for transplanting

T. capillaris individuals for transplanting and controls were collected in May 2012 in a canyon in the vicinity of La Paz (16°31′31.60″S; 68°03′36.43″W). This location is far from atmospheric metal(loid) fallout, but has similar geographical and meteorological conditions as the transplantation sites. Whole plant samples were collected with plastic gloves to avoid contamination by metal(loid)s, as reported in previous active biomonitoring studies using *T. capillaris* (Goix et al., 2013; Bermudez et al., 2009). Three groups of three *T. capillaris* individuals were collected in the same canyon but not transplanted: these were used as controls without metal exposure due to transplantation and monitoring experiments.

2.2. Transplantation, time-dependent sampling and collection of natural specimens

The exposure experiment was performed in Oruro City (17°58′S–67°60′W), in the Bolivian Altiplano region, in the Andean Cordillera oriental, at an altitude of 3700 m above sea level, from June to November 2012. According to Goix et al. (2011,2013), weather conditions in this region are typical of the Bolivian Altipano: semi-arid and cold (*i.e.*, mean annual rainfall of 366 mm and average temperature of about 12 °C). Two seasons can be differentiated: a short wet season from November to January, accounting for about 63% of annual rainfall, and a long dry and colder season from February to October. The city of Oruro is well-known for its polymetallic mining activities and its large Sn smelter complex (Goix et al., 2013). Previous studies reported that pollution sources and air particulate matter (PM) levels vary in the different districts of the city (Goix et al., 2011; Cadot et al., 2013). Thus, three zones of interest were identified and used for time-dependent experiments: (i) The *San José district noted "Mine"*, in the vicinity of the mine producing, in decreasing order, approximately 30,000 t of Zn, 10,000 t of Sn, 2500 t of Pb, 500 t of Sb, 130 t of Ag and W, 45 t of Cu and 2.5 t of Au yearly (Instituto Nacional de Estadística, 2010), (ii) The *Vinto district noted "Smelter"*, where smelting activities and production of Sb and Sn takes place, along with Bi, Ag and Pb produced as secondary elements, and (iii) *Downtown Oruro*, characterized by high residential density, urban activities, traffic and a few industries, with lower pollution levels (Goix et al., 2011).

T. capillaris plants were thus exposed in these three zones (Fig. SI-1): Mine (17°57′38.88″S; 67°07′03.91″W), Smelter (17°58′42.57″S; 67°03′02.11″W) and Downtown Oruro (17°58′08.36″S; 67°07′03.91″W). Plants were exposed in nylon

mesh bags: three individuals per bag for a total of 50 g of *T. capillaris* per bag. Six bags were exposed in June in each zone, using trunks or stakes with small plastic cable ties, at 3 m in height to better catch air pollution. From July 2012 to December 2012, a mesh bag was taken off on the 10th day of every month, and used for the time-dependent analysis (plants were weighed before and after the exposure period). In parallel to the experiment with transplanted specimens, natural specimens were collected at the Mine and Downtown sites. No natural specimens were found in the smelter area. A washing procedure was used to remove adherent particles present on the plant surfaces (Goix et al., 2013; Smodiš et al., 2004). Each plant was placed in ultrapure water, sonicated for 3 min and rinsed again. Then plants were dried at 40 °C for 48 h and ground in an agate mortar in liquid N_2. Ground plant samples were then dried again for 48 h and stored in polyethylene vials (Goix et al., 2013). Separate aliquots of plant samples were kept fresh and prepared as frozen hydrated samples for XAS.

At each location, passive filters (Whatman, QMA, Quartz fiber) of $14 \times 9\,cm^2$ area were exposed next to the *Tillandsia* bags, at 3 m high, under the same conditions as the plants, and collected according to the same protocol for time-dependent analyses. However, passive filters were not washed before digestion or XAS analysis.

2.3. Determination of total metal(loid) concentrations in plants and filters

The washed *T. capillaris* samples and non-washed filters from the 5-month exposure experiment were digested and analyzed. For each sample, 100 mg of *T. capillaris* or filter was precisely weighed with a digital balance (precision of 10^{-4} g) before acid digestion. Samples were placed into pyrex liners with Teflon skirts and 1 mL suprapur® H_2O_2, 3 mL bi-distilled HNO_3 (15 N) added. The samples were sonicated for 45 min and then incubated at 60 °C for 8 h. Then, 3 mL bi-distilled HNO_3 (15 N), 4 mL HCl and 0.3 mL 48% suprapur® HF were added and the samples were heated at 60 °C for another 8 h. Mixtures were then heated in a CEM Discover® microwave accelerated reaction system (heating at 130 °C with 7 min ramp time, 1 min hold time, heating at 160 °C with 5 min ramp time, 1 min hold time, heating at 180 °C with 5 min ramp time, 10 min hold time) before evaporation in a clean fume-hood (72 h at 70 °C). Each microwave mineralization run contained 10 samples, one blank and one certified reference material sample (BCR-482, lichen standard). After complete evaporation, the remaining solid residue for each sample was dissolved in 20 mL of a 10% HNO_3/0.05% HF acidic mixture to prevent Sn precipitation (Goix et al., 2013).

Metals and metalloids (Ag, As, Cd, Cr, Cs, Cu, Pb, Sb, Sn, U, W and Zn) were measured with the Thermo-Finnigan Agilent® 7500ce Inductively Coupled Plasma Mass Spectrometer (ICP-MS) using an In-Re internal standard spike to correct data for instrumental drifts and plasma fluctuations. Quality assurance and measurement traceability were ensured by measuring five replicates of BCR-482 for *T. capillaris* and NIST SRM 1648 "Urban Particulate Matter" for aerosols deposited on passive filters. The detection limits were approximately 20, 2, 0.1, 1, 7, 4, 1, 500, 5, 0.1, 100 and 10 ng g^{-1} for Ag, As, Cd, Cr, Cs, Cu, Pb, Sb, Sn, U, W and Zn, respectively. Recoveries were expressed as the ratio of the measured to certified concentrations: relative standard deviations (RSD%) were <5%, and relative standard deviation on blanks replicates was <10%. Metal(loid) concentrations are expressed in dry weight (mg kg^{-1}, DW). All certified elements presented satisfying recoveries, in the 92.2–102.4% range (92.2% for Cr and 102.4% for Ag) as already reported by Goix et al. (2011, Table B1).

Total Hg concentrations in *T. capillaris* were determined by atomic absorption spectrophotometry (Guédron et al., 2013) following catalytic decomposition and gold amalgamation with an automatic mercury analyzer (Altec, AAS Model AMA 254). The relative precision was ±10% as determined from triplicate measurements of certified reference materials (CRM). Concentrations obtained for repeated CRM analyses never exceeded the published concentration range (0.090 ± 0.012 mg kg^{-1} and 0.091 ± 0.008 mg kg^{-1} for CRMs 7002, and MESS-3, respectively). The detection limit, defined as three times the standard deviation of the blank, was 0.005 mg kg^{-1}.

2.4. Morphological observations and identification of metal-enriched particles using SEM-EDX

Environmental SEM-EDX measurements using a Jeol JSM 6360LV instrument equipped with a PGT Sahara EDX Silicon Drift Detector (SDD) were carried out to investigate epiphyte morphology, trichome conformation and elemental distribution of the metal-enriched areas. Before analysis, *T. capillaris* plants were dried and fixed on a carbon substrate without any further preparation. The apparatus was operated in low-vacuum mode (~133 Pa) at 25 kV. Observations were performed on plant fragments exposed for 1 month (from June 10 to July 10) in the Smelter district (with high contamination levels) and after a washing process.

2.5. Study of Pb and As speciation in T. capillaris using X-ray absorption spectroscopy (XAS)

Samples investigated by XAS to assess As and Pb speciation included slag particles from Vinto smelters, passive filters containing atmospheric particles, *T. capillaris* natural specimens collected on site, and transplanted specimens (Table SI-1 in Supporting Information). For one sample (*T. capillaris* transplanted at the Smelter site), spectra for both washed and unwashed plants were recorded and compared. Filters were cut into 5-mm diameter discs, and five were superimposed and placed in the XAS sample holder. The plant and slag samples were ground and pressed into 5 mm diameter pellets. Lead reference compounds included: metallic Pb, PbS, $PbSO_4$, α- and β-PbO, $PbCO_3$, PbO_3S_2, $Pb_3(OH)_2(CO_3)_2$, pyromorphite $Pb_5(PO_4)_3Cl$ (Sigma–Aldrich) and three metal sulfide samples originating from the Oruro mine (Purchased from David H. Garske, Tucson, USA). Based on X-ray diffraction, Oruro mine samples contained mixed sulfides belonging to the sulfosalt family. The first sample contained franckeite ($Pb_5Sn_3Sb_2S_{14}$), the second franckeite and jamesonite ($Pb_4FeSb_6S_{14}$), and the third one jamesonite and andorite ($PbAgSb_3S_6$). The following solid sorbed and complexed Pb species were also used as Pb standards: Pb sorbed onto ferrihydrite containing 2% weight Pb prepared at pH 7.3, Pb sorbed onto birnessite containing 2% weight Pb prepared at pH 6.5 and Pb pectin containing 0.8% weight Pb. Finally, aqueous Pb reference compounds included free Pb^{2+} (20 mM $Pb(NO_3)_2$, pH 4.0), Pb citrate (10 mM $Pb(NO_3)_2$, 100 mM Na citrate, pH 5.4), and Pb malate (10 mM $Pb(NO_3)_2$, 100 mM Na malate, pH 5.0). Arsenic reference compounds included arsenopyrite ($FeAs^{III}S$), $As^{III}{}_2S_3$, $As^{III}{}_2O_3$, As^{III} bound to glutathione (As^{III}-GSH) (Langner et al., 2012), As^V sorbed on calcite, FeS, FeS_2, goethite and ferrihydrite (Couture et al., 2013), and monothio As^V and tetrathio As^V sorbed on FeS, FeS_2, goethite and ferrihydrite (Couture et al., 2013), and $Na_2HAs^VO_4$. Lead and As reference compounds were prepared as pellets diluted in BN or not, or as frozen liquids after mixing with glycerol (20% in volume), as described previously (Schreck et al., 2014).

XAS experiments were performed on beamline BM30B (FAME) at the European Synchrotron Radiation Facility (ESRF, Grenoble, France). The beamline was equipped with a Si(111) double crystal monochromator, a 30-element solid state Canberra detector for fluorescence mode and a diode for transmission mode. All spectra were recorded using a He cryostat cooled at 10 K. The XAS spectra of Pb L_{III}-edge and As K-edge were recorded in transmission or fluorescence mode, depending on their concentration. Two to

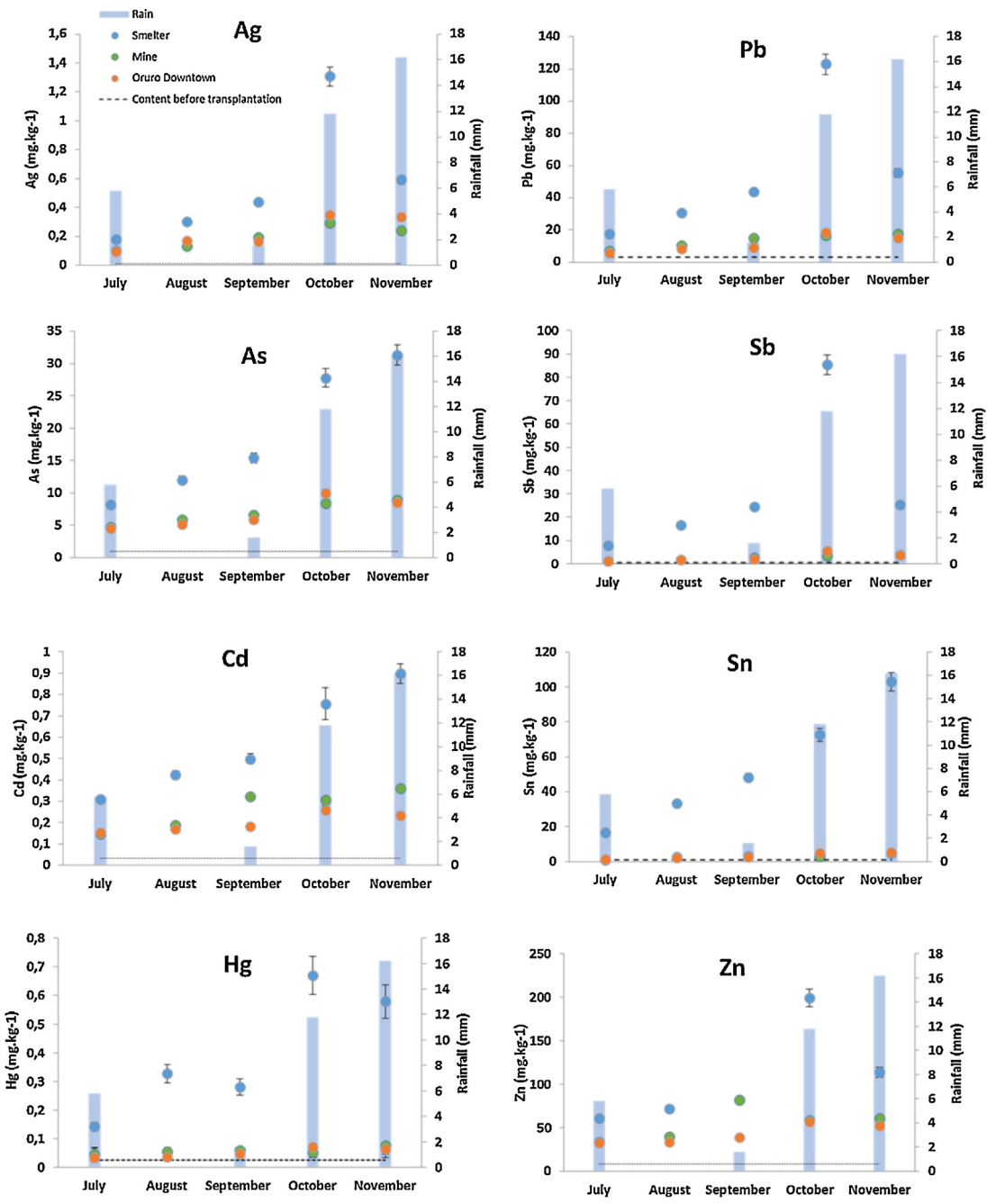

Fig. 1. Metal(loid) concentrations in transplanted *T. capillaris* as a function of the exposure time (in months). Vertical bars indicate rainfall (mm) during the same period.

six spectra of 45 min for Pb and 20 min for As were recorded for each sample, and the beam was moved between each spectrum to limit possible radiation damage. For spectra recorded in fluorescence mode, data from each detector channel were inspected for glitches or dropouts before inclusion in the final average.

XAS data was extracted using ATHENA software (Ravel and Newville, 2005). Pb and As XANES spectra were calibrated by taking the inflection point of metallic Pb at 13035.0 eV and of $Na_2HAs^VO_4$ at 11,873.4 eV, respectively. Principal component analysis (PCA) was not used for Pb XANES and EXAFS spectra because the set of spectra was too limited. These spectra were treated by linear combination fits (LCFs) using up to three components from the list of standard spectra cited above. Normalized As XANES spectra were treated by PCA and LCFs of reference compound spectra. For all LCFs, the quality of the fits was evaluated using the normalized sum-squares residuals. For XANES spectra analysis, no E_0 shift or slope correction was allowed.

3. Results and discussion

3.1. Comparison of total metal(loid) concentrations in T. capillaris and passive filters

The evolution of the metal(loid) concentrations in *T. capillaris* transplanted to and exposed at the three sites is shown in Fig. 1. Overall metal concentrations decreased in the order: Zn > Pb > Sn > Sb > As > Ag > Cd > Hg, regardless of the month. After normalization with uranium (not shown), a similar pattern was observed for *T. capillaris* exposed for a longer period in the same area (Goix et al., 2013). The results showed that the sampling

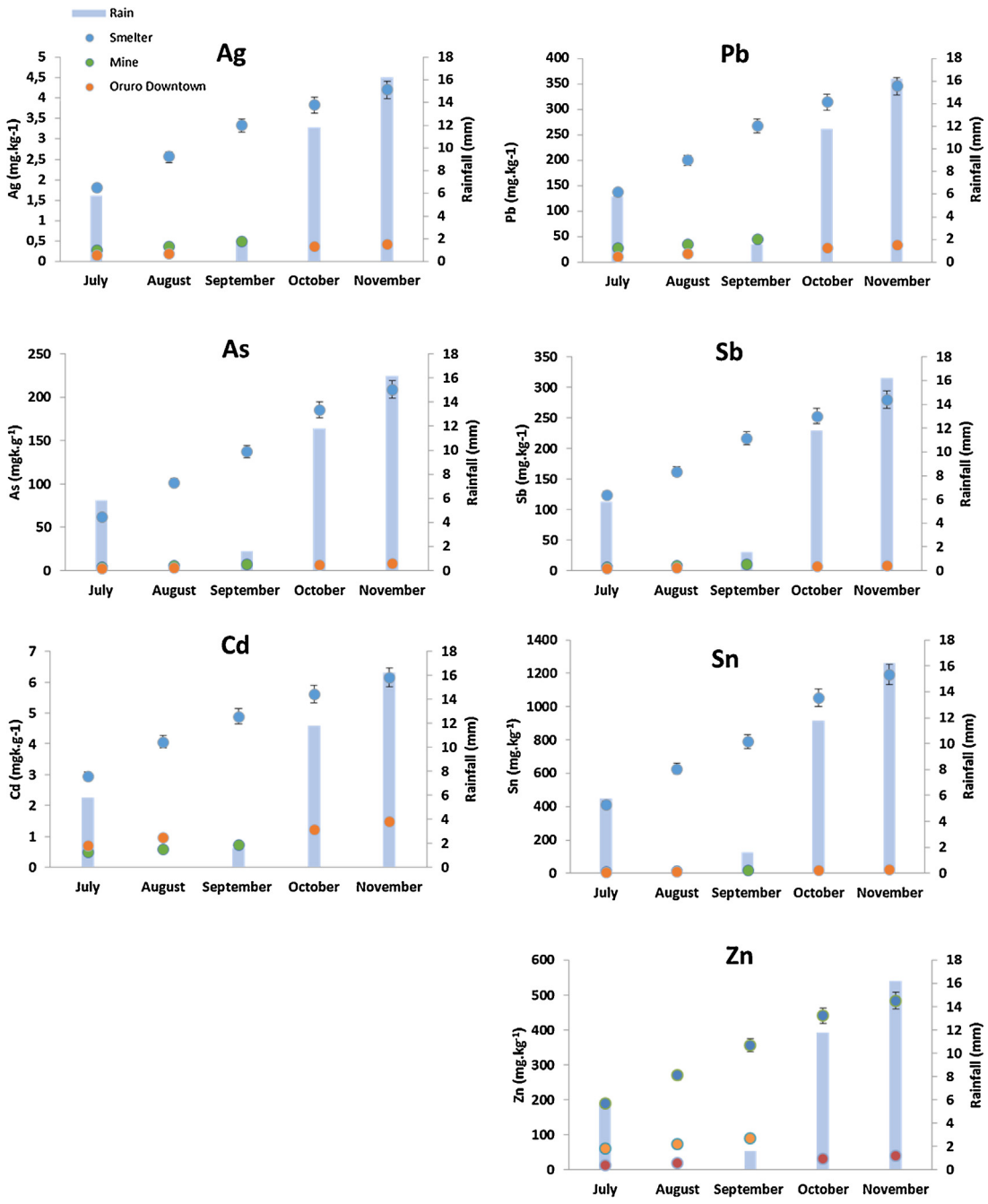

Fig. 2. Metal(loid) concentrations in passive filters as a function of the exposure time (in months), and rainfall (mm) during the same period.

location had a clear influence on the concentrations: Ag, Hg, Pb, Sb, Sn, and Zn concentrations in plants from the Smelter area were twice as high as those from the Mine and Downtown Oruro samples. This observation is consistent with PM_{10} measurements. PM_{10} concentrations throughout the experiment were 65 $\mu g\,m^{-3}$ in the Smelter area compared to 31 $\mu g\,m^{-3}$ and 35 $\mu g\,m^{-3}$ in the Mine and Downtown sites, respectively. These data confirm that the Sn smelter has a major impact on atmospheric metal(loid) contamination in the area.

For the Smelter area, the As, Cd and Sn concentrations increased regularly from July to November. Mercury showed a sharp increase from September to October, dropped for a month, and stabilized in November. The absence of significant Hg accumulation at the two other sites indicates that the smelter is the major source of Hg in Oruro. Mercury could still have come from other sources such as coal burning, traffic, Au–Hg amalgamation in the gold mines of the region, and global deposition but are not likely to be relevant at a six-month timescale. Mercury can be emitted as particulate Hg (mainly Hg(II) associated with particles) or in its gaseous form (Hg(0)). In the present study, it was not possible to evaluate the proportion of each one. The concentrations of Ag, Sb, Pb and Zn reached a maximum in October and decreased slightly in November. Maximum levels of element incorporation in *Tillandsia* species vary among studies. For example, Martínez-Carrillo et al. (2010) and Isaac-Olivé et al. (2012) found a maximum of accumulation after 6-10 weeks for *T. Usneoides*. Whereas, in the study of Bermudez et al. (2009), focusing on three different species of Tillandsias, the maximum accumulation was after six months. In the present study, the decrease could not be attributed to plant growth since this would have affected all elements. Fig. 2 shows the metal(loid)

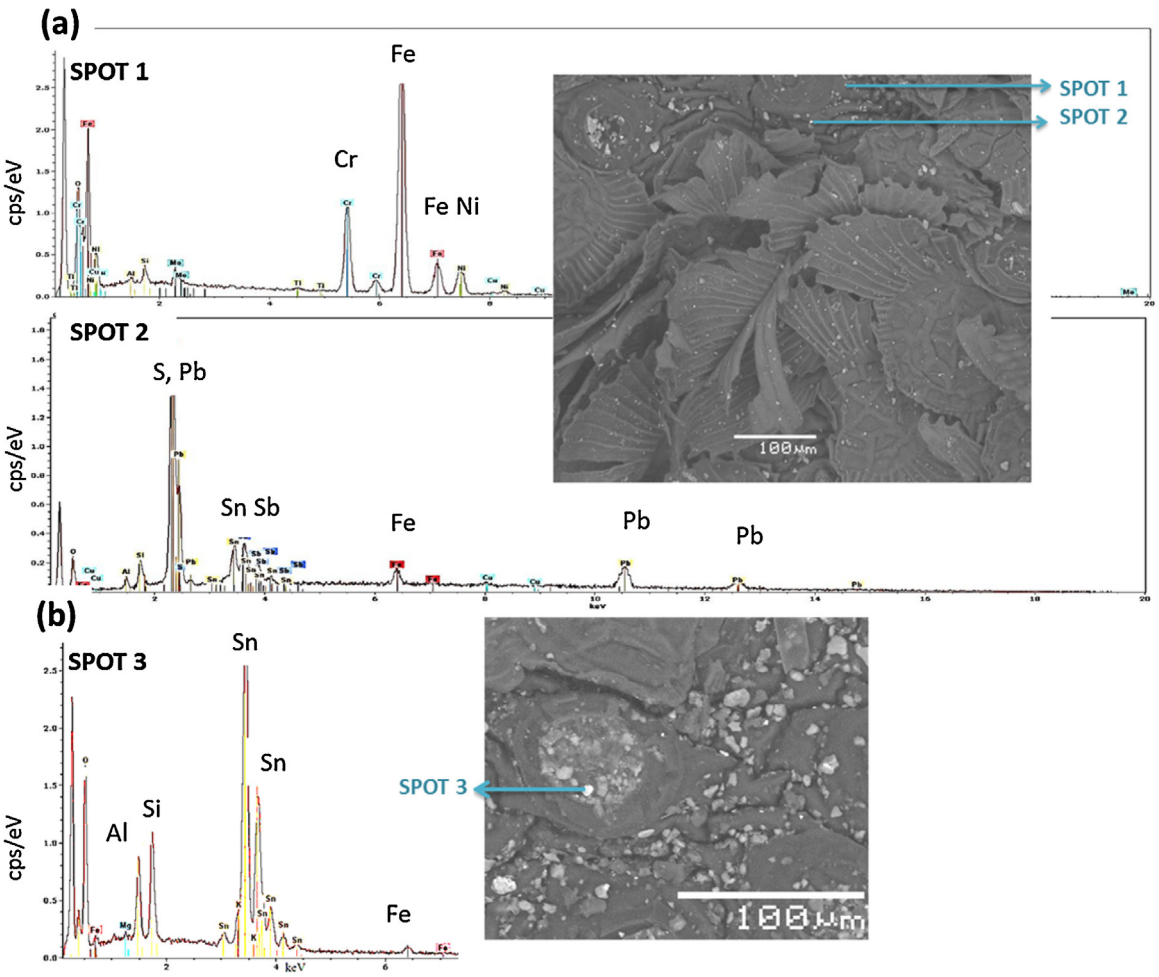

Fig. 3. SEM-EDX images and associated spectra of *T. capillaris* exposed to atmospheric fallout (Mine district, after two months of exposure). Typical trichome area containing metal(loid) enriched particles; (b) Zoom in on particles deposited in or near a stomata (after trichome aisle destruction).

concentrations from the passive filters, as a function of the exposure time (in months) and rainfall (mm), subjected to the same exposure conditions in the Smelter area and during the same period (June to November 2012). All the studied metals and metalloids increased with time in the passive filters. Thus, these results suggest that the decrease in Ag, Sb, Pb and Zn concentrations in Tillandsias in November was not due to their decreased deposition from rainfall cleaning up the air (Fig. 2).

A possible hypothesis is the preferential leaching of some elements present on the plant's surface, possibly due to different types of interactions between the particles or metals and the plants. The leaching process can be an important factor leading to a decrease in more soluble elements in the plant. However, as rainfall leaching is a physical process, which should occur in exactly the same manner in passive filters as in *T. capillaris*. Thus, the reduced metal concentrations in plants could certainly be explained by some changes in speciation and solubility of different metallic phases after deposition on the plant surface in the wet periods. A seasonal rain-washing effect was proposed in previous biomonitoring studies using *Tillandsia* species (Wannaz and Pignata, 2006; Bermudez et al., 2009; Bermudez and Pignata, 2011; Abril et al., 2014). The comparison between *T. capillaris* and the passive filters suggests that atmospheric metal contaminants accumulate more linearly as a function of time in filters than plants, especially in wet periods. For the plants and passive filters from the Mine and Downtown area, no significant increases in metal(loid) concentrations were observed in the five-month exposure. Thus, neither *T. capillaris* transplants or passive filters are efficient monitors of moderate atmospheric contamination for this time period.

3.2. *Plant morphology and particle localization in* T. capillaris

Fig. 3 shows SEM images of *T. capillaris* exposed to atmospheric fallout and their associated EDX spectra. Typical trichome structures were observed (Fig. 3a). Metal(loid)-rich particles of various shapes and sizes were observed on the plant surface. EDX analyses showed high concentrations of Pb and Sn, plus other metals including Cu, Fe, and Zn depending on the particles. Al, S and Si were also present in some grains. On the basis of these analyses, the major minerals appear to be metal oxides and sulfides, and aluminosilicates. Trapped particles could be observed by focusing on the central shield with the disc cells after trichome aisle destruction (Fig. 3b), suggesting that central disc cells could be a pathway for the incorporation of metal particles in plants. The channel formed by stalk cells between the central disc cells and the mesophyll cells, which is used for absorption of water and macronutrients, could be a pathway for metal uptake, as observed for Cs by Li et al. (2012). SEM-EDX is not sensitive enough to detect diffuse metal concentrations. Thus, to obtain further insights into the fate of metal(loid)s in *T. capillaris*, the speciation of two Pb and As was studied in the slag, in passive filters and in plants by XAS.

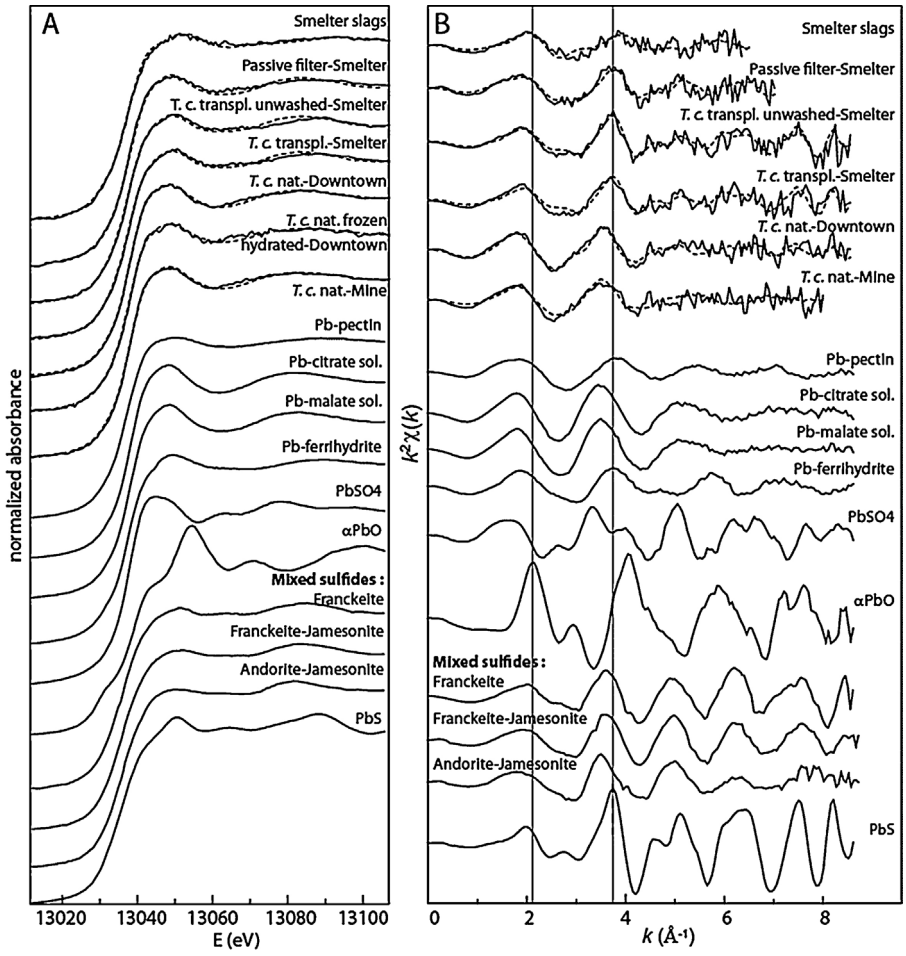

Fig. 4. Pb L_{III}-edge XANES (A) and EXAFS (B) spectra for Pb reference compounds and samples from Oruro (solid lines), and linear combination fits (dashed lines).

3.3. *Pb and As speciation in* T. capillaris *and passive filters and the possible mechanisms involved*

Lead and As speciation was studied in passive filters, in *T. capillaris* samples transplanted in the Smelter area (natural specimens were absent in this location) and *T. capillaris* growing naturally in Mine and Downtown locations (the Pb content in transplanted specimens was too low for XAS).

Fig. 4 shows the Pb L_{III}-edge XANES and EXAFS spectra for Pb reference compounds including some mixed metal sulfides from Oruro ore (franckeite, jamesonite and andorite, present as pure phases or as mixtures), for the Smelter slags, for a passive filter from the Smelter area, and for *T. capillaris* samples. The proportion of Pb species in each sample was determined by LCFs of XANES and EXAFS spectra (Fig. 4 and Fig. SI-2). LCF results obtained based on the XANES and EXAFS data were consistent within 10% error. Three families of Pb species were identified in the LCFs: (i) Pb sulfides (galena (PbS) and/or mixed metallic sulfides), (ii) α-PbO, and, (iii) sorbed Pb and/or Pb–organic complexes. Fits of similar quality were obtained with either sorbed Pb or Pb–organic complexes, which do not have a very distinctive EXAFS signature; hence these species were merged in a single pool. The reference used as the sorbant phase was ferrihydrite, a proxy for Pb sorbed on various types of oxides and oxyhydroxides. Lead speciation in the Smelter slags was fitted with a combination of α-PbO and sorbed and/or Pb–organic acid complexes. The presence of Pb oxides in Smelter slags was observed previously (Thiry et al., 2002; Ettler et al., 2005, 2006, 2009a,b). Other Pb species typical of slags, including PbS and metallic Pb, were not observed here. These species may have been altered during manipulation and stockpiling of the slag. Sorbed Pb species and Pb sulfate-containing species may result from the alteration of Pb oxides and sulfides and metallic Pb, generally trapped in the glassy matrix. Lead-organic acid complexes are less likely because of the low organic matter content in the slag. *T. capillaris* and the passive filters from the Smelter area contained a mixture of Pb sulfides (galena or mixed sulfides) and of sorbed Pb and/or Pb–organic acid complexes.

Lead sulfides were observed in smelter samples only (filter and plant samples exposed for five months). They likely come from atmospheric fallout from the smelter. Smelters processing metal sulfides generally emit a mixture of metal sulfides, sulfates, oxysulfates and oxides (Batonneau et al., 2004). In addition, these minerals may have come from ore, manipulated close to the smelter. Indeed, large amounts of ore are transported to the smelter from the San José mine and from other mines in the country and manipulated mechanically at the smelter. These operations generate significant PM emissions into the atmosphere. The absence of Pb sulfides in natural plants collected at the Mine and Downtown sites may suggest their absence in PM in these areas, or their weathering over time due to a longer exposure time. Based on their size, these specimens have probably been exposed for several years. Secondary species present in the passive filter (sorbed Pb) and in the plants (sorbed Pb and/or Pb–organic complexes) may result from the oxidation of primary minerals (Pb, PbS, PbO) and/or physiological processes for Pb–organic complexes in the plant. Their proportion was slightly higher in the passive filters than in the transplant from the Smelter site (Table 1). This comparison suggests that plant-trapped particles are more protected from weathering/oxidation

Table 1
Distribution of Pb species as determined by LCFs of Pb L_{III}-edge XANES and EXAFS spectra.

Sample	Location	Date of collection		Distribution of Pb species (in molar %)				
				Pb sulfides[a]	α-PbO	Sorbed and/or complexed Pb species[b]	Sum	*NSS*[c]
Slags	Smelter		XANES		19	29	48	5.55E−01
			EXAFS		25	85	110	1.76E−04
Passive filter	Smelter	Oct.	XANES	30		70	100	2.09E−04
			EXAFS	21		65	86	4.97E−01
T.c. transpl. unwashed	Smelter	Oct.	XANES	46		54	100	1.85E−04
			EXAFS	30		51	81	3.39E−01
T.c. transpl.	Smelter	Oct.	XANES	42		58	100	1.40E−04
			EXAFS	29		57	86	3.80E−01
T.c. nat.	Downtown		XANES			100	100	9.00E−05
			XANES (froz. hydr.)			100	100	2.00E−04
			EXAFS			65	65	3.03E−01
T.c. nat.	Mine		XANES			100	100	1.20E−04
			EXAFS			61	61	3.75E−01

[a] Including galena (PbS) and mixed sulfides.
[b] Fitted with Pb–organic acid and Pb–pectin complexes, and Pb sorbed on ferrihydrite.
[c] Normalized sum-squares residual $NSS = \sum(\mu_{experimental} - \mu_{fit})^2(\mu_{experimental})^2 \times 100$ in the 13015–13110 eV range for XANES, and $NSS = \sum(\chi k^2{}_{experimental} - \chi k^2{}_{fit})^2(\chi k^2{}_{experimental})^2 \times 100$ in the 0–7 to 0–9 $Å^{-1}$ range for EXAFS.

than particles trapped in the filter. Finally, Pb speciation did not differ significantly between washed and unwashed plants. Thus, rinsing with water did not significantly modify Pb-rich particles. *T. capillaris* plants growing naturally in the vicinity of the Mine and Downtown Oruro did not contain Pb sulfides, and only sorbed and/or Pb–organic acid complexes were measured. Thus, sulfides and oxides identified by SEM-EDX in *T. capillaris* did not represent major Pb species, and secondary forms including sorbed Pb and/or Pb–organic complexes were identified with EXAFS. These species may correspond to Pb-cell wall complexes, as observed for other plant species exposed to Pb (Tian et al., 2010).

PCA could be used to interpret As speciation because a larger set of samples was studied using As K-edge XANES spectroscopy (Fig. 5, Table SI-1). The set of spectra was described by four components (see Table SI-2 and Fig. SI-3). The following species were correctly reconstructed using target transformation: $As^{III}S$, $As^{III}{}_2O_3$, $MTAs^{V}$=FeS, $TTAs^{V}$=FeS, and various As^{V} species (Fig. 5, Table SI-3 in supporting information). The species $MTAs^{V}$=FeS, $TTAs^{V}$=FeS

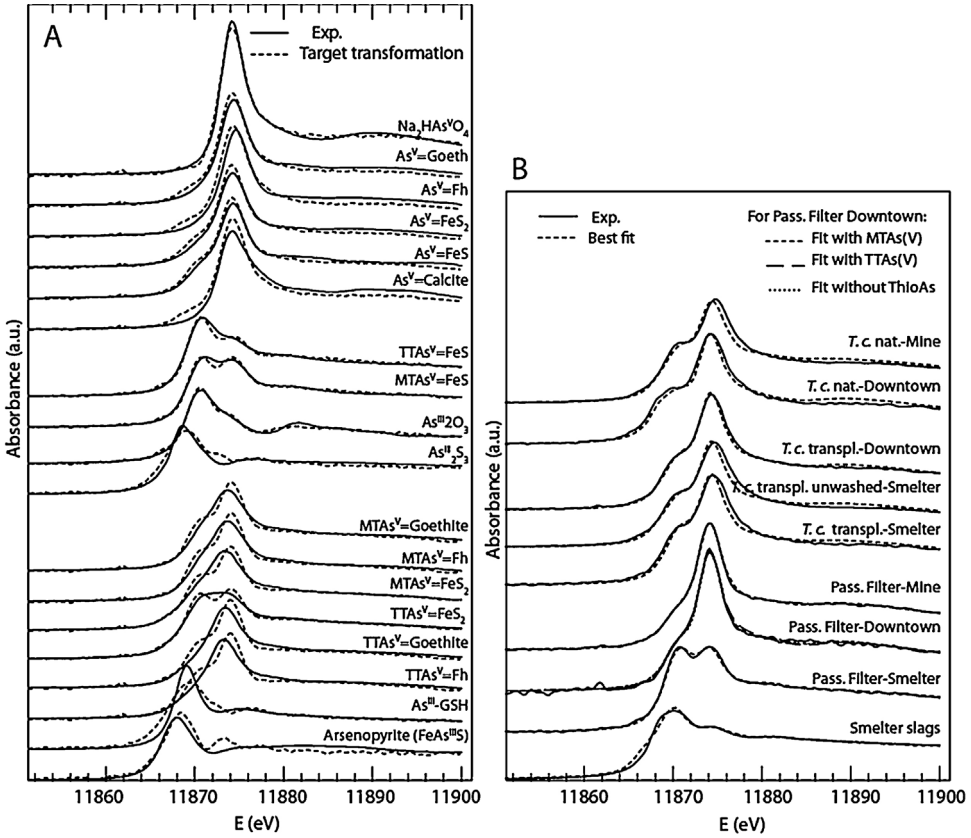

Fig. 5. Arsenic K-edge spectra for (A) the reference compounds (solid lines) and target transformation using four components (dashed lines) (the six spectra at the bottom of the figure are not correctly reproduced), and (B) for Oruro samples (solid lines) and their linear combination fits (dashed lines).

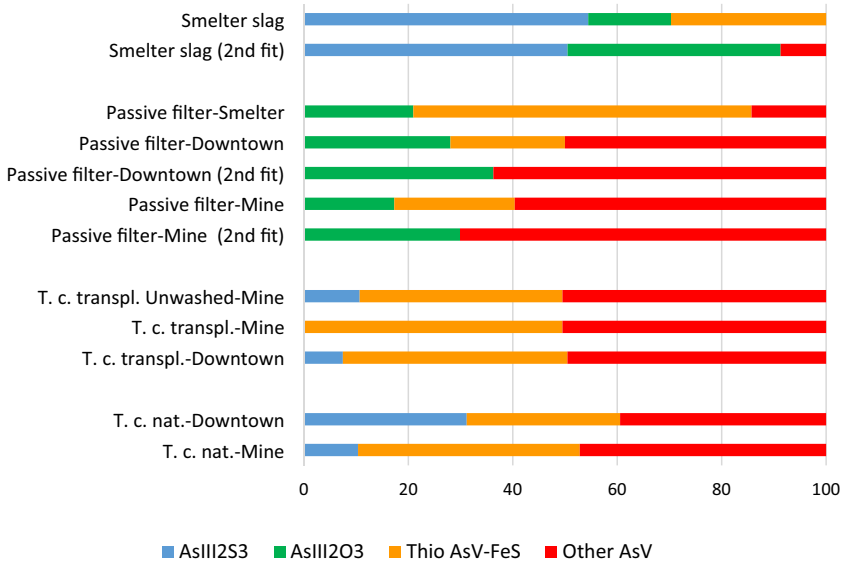

Fig. 6. Proportion of As species determined by LCFs in the Oruro samples. Percentages presented in Table SI-4 were normalized to 100%, and MTAsV=FeS and TTAsV=FeS species were merged as thioAsV=FeS.

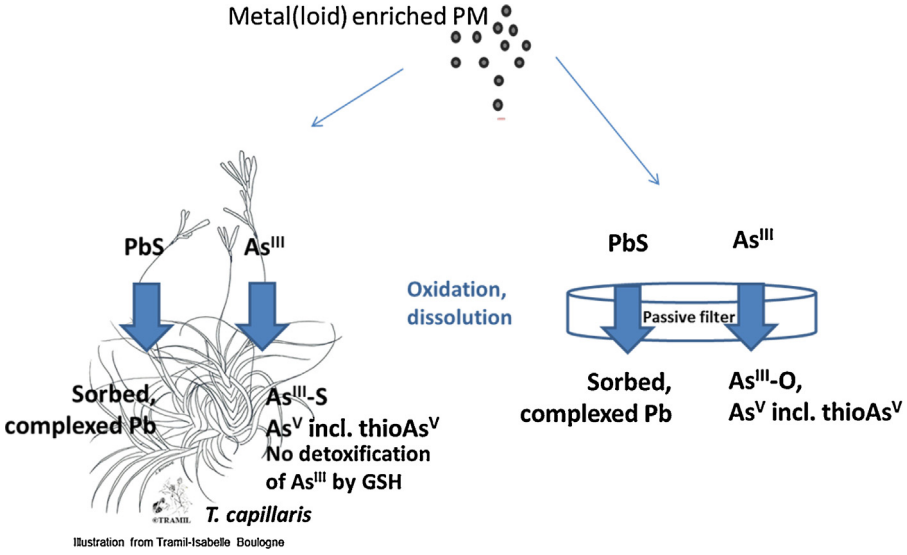

Fig. 7. Metal(loid) dynamics in *T. capillaris vs* passive filters.

have relatively similar XANES signatures, although MTAs^{V}=FeS has a higher shoulder at 11,874 keV (Fig. 5). Thus, they were merged as "TAs^{V}=FeS" in the LCFs. Interestingly, arsenopyrite was not identified as a component, although this species was identified in minerals from the mine (data not shown). Likewise, As^{III}GSH, which could have been indicative of a detoxification process in the plant, could not be reconstructed.

LCFs were carried out using up to four components among these species (Figs. 5 and 6 and Table SI-3). For some spectra, fits with and without TAs^{V}=FeS were obtained, so two distributions are shown in Fig. 6. In the slag, the majority of As species were reduced (sulfide or oxide) and it contained 10–30% As^{V}. All other samples (passive filters and plants) contained a majority of oxidized As species.

Smelters are known to emit both As^{III} and As^{V} species (Sanchez de la Campa et al., 2008), whereas PM from other origins mostly contains As^{V} (Godelitsas et al., 2011). The thio-As^{V} species was possibly present in slag and passive filters exposed at the Downtown and Mine sites, and it was clearly identified in passive filters from Smelter and in all plant samples. This species can result from the oxidative dissolution of As-bearing sulfide minerals (Suess and Planer-Friedrich, 2012). As^{III} sulfide was detected in plants whereas passive filters contained As^{III} oxide. Non-hyperaccumulating species were previously reported to detoxify As by chelation with thiol containing molecules such as phytochelatins (Sarret et al., 2013; Zhao et al., 2009). In the present case, As^{III}GSH, which can be considered as a proxy for As^{III}-thiol species, was not detected in the plant samples. The fate of metal particles trapped in *T. capillaris* and passive filters and their possible origin are summarized in Fig. 7.

4. Conclusions

We monitored metal(oid) accumulation in passive filters and transplanted *T. capillaris* at three sites in an urban mining area in Bolivia for five months. A linear increase in all metals and metalloids was observed in the filters. The evolution of metal(oid) content in *T. capillaris* was relatively consistent with that of the passive filters in the highly contaminated area, with the exception of Ag, Pb,

Sn and Zn, which decreased in the fifth month. As rainfall leaching is a physical process, occurring in exactly the same manner in passive filters as in *T. capillaris*, this decrease suggests that binding mechanisms by plants and filters are different for those elements. This also suggests possible excretion by the plant, although further studies would be needed to test this hypothesis. For the moderately contaminated zone, the 5-month exposure time was not sufficient for either plants or filters to accumulate contaminants. Thus, the exposure time needs to be optimized at each site, and weather conditions should be taken into account. Natural specimens were two- to four-fold richer in metals and metalloids than transplants. Although no calibration is possible for natural samples, they can be used to get a rough idea of the contamination in a given area, and to detect low contaminant levels. Evidence of chemical transformation was found for Pb and As in both plant samples and filters. For Pb, primary species were progressively replaced by sorbed Pb and/or cell wall complexes. Arsenic underwent oxidation from As^{III} to As^{V} species, with the persistence of a minor fraction of As^{III} sulfide in plants and As^{III} oxide in filters. The release of some metals by the plant and the sorption of Pb to the cell walls could be related to detoxification mechanisms, however more data are needed to make further conclusions on this point.

Acknowledgements

We are grateful to ESRF for providing beam time and to the FAME beamline staff for their help in collecting data. This work was funded by the CNRS/INSU/EC2CO AEROBOL 2012-2014 program, and Labex OSUG@2020 (Investissements d'avenir – ANR10 LABX56). We thank Valentin Perraux for chemical analyses at ISTerre. Finally, we want to sincerely thank Leigh Gebbie for her help in English language review.

Appendix A. Supplementary data

Supplementary data associated with this article can be found, in the online version, at http://dx.doi.org/10.1016/j.ecolind.2016.02.027.

References

Abril, G.A., Wannaz, E.D., Mateos, A.C., Pignata, M.L., 2014. Biomonitoring of airborne particulate matter emitted from a cement plant and comparison with dispersion modelling results. Atmos. Environ. 82, 154–163.

Amado Filho, G.M., Andrade, L.R., Farina, M., Malm, O., 2002. Hg localisation in *Tillandsia usneoides L* (Bromeliaceae), an atmospheric biomonitor. Atmos. Environ. 36, 881–887.

Ares, A., Aboal, J.R., Carballeira, A., Giordano, S., Adamo, P., Fernández, J.A., 2012. Moss bag biomonitoring: a methodological review. Sci. Total Environ. 432, 143–158.

Batonneau, Y., Bremard, C., Gengembre, L., Laureyns, J., Le Maguer, A., Le Niaguer, D., Perdrix, E., Sobanska, S., 2004. Speciation of PM_{10} sources of airborne nonferrous metals within the 3-km zone of lead/zinc smelters. Environ. Sci. Technol. 38, 5281–5289.

Bermudez, G.M.A., Rodriguez, J.H., Pignata, M.L., 2009. Comparison of the air pollution biomonitoring ability of three *Tillandsia* species and the lichen *Ramalina celastri* in Argentina. Environ. Res. 109, 6–14.

Bermudez, G., Pignata, M., 2011. Antioxidant response of three *Tillandsia* species transplanted to urban, agricultural, and industrial areas. Arch. Environ. Contam. Toxicol. 61, 401–413.

Cadot, E., Ruiz-Castel, M., Barbieri, F., Paco, P., Goix, S., Gardon, J., 2013. Les déterminants individuels de l'exposition humaine au plomb. Une analyse de la cohorte ToxBol, Oruro, Bolivie. Rev. d'Épidémiol. Santé Publ. 61, 111–112.

Carreras, H.A., Wannaz, E.D., Pignata, M.L., 2009. Assessment of human health risk related to metals by the use of biomonitors in the province of Córdoba, Argentina. Environ. Pollut. 157, 117–122.

Couture, R.M., Rose, J., Kumar, N., Mitchell, K., Wallschläger, D., Van Cappellen, P., 2013. Sorption of arsenite, arsenate, and thioarsenates to iron oxides and iron sulfides: a kinetic and spectroscopic investigation. Environ. Sci. Technol. 47, 5652–5659.

Ettler, V., Vaněk, A., Mihaljevič, M., Bezdička, P., 2005. Contrasting lead speciation in forest and tilled soils heavily polluted by lead metallurgy. Chemosphere 58, 1449–1459.

Ettler, V., Mihaljevič, M., Šebek, O., Molek, M., Grygar, T., Zeman, J., 2006. Geochemical and Pb isotopic evidence for sources and dispersal of metal contamination in stream sediments from the mining and smelting district of Příbram, Czech Republic. Environ. Pollut. 142, 409–417.

Ettler, V., Vrtišková, R., Mihaljevič, M., Šebek, O., Grygar, T., Drahota, P., 2009a. Cadmium, lead and zinc leaching from smelter fly ash in simple organic acids – simulators of rhizospheric soil solutions. J. Hazard. Mater. 170, 1264–1268.

Ettler, V., Johan, Z., Kříbek, B., Šebek, O., Mihaljevič, M., 2009b. Mineralogy and environmental stability of slags from the Tsumeb smelter, Namibia. Appl. Geochem. 24, 1–15.

Figueiredo, A.M.G., Nogueira, C.A., Saiki, M., Milian, F.M., Domingos, M., 2007. Assessment of atmospheric metallic pollution in the metropolitan region of São Paulo, Brazil, employing *Tillandsia usneoides* L. as biomonitor. Environ. Pollut. 145, 279–292.

Fontúrbel, F.E., Barbieri, E., Herbas, C., Barbieri, F.L., Gardon, J., 2011. Indoor metallic pollution related to mining activity in the Bolivian Altiplano. Environ. Pollut. 159, 2870–2875.

Gao, H., Chen, J., Wang, B., Tan, S.C., Lee, C.M., Yao, X., Yan, H., Shi, J., 2011. A study of air pollution of city clusters. Atmos. Environ. 45, 3069–3077.

Godelitsas, A., Nastos, P., Mertzimekis, T.J., Toli, K., Simon, R., Gottlicher, J., 2011. A microscopic and synchrotron-based characterization of urban particulate matter (PM10-PM2.5 and PM2.5) from Athens atmosphere, Greece. Nucl. Instrum. Methods Phys. Res. B 269, 3077–3081.

Goix, S., Point, D., Oliva, P., Polve, M., Duprey, J.L., Mazurek, H., Guislain, L., Huayta, C., Barbieri, F.L., Gardon, J., 2011. Influence of source distribution and geochemical composition of aerosols on children exposure in the large polymetallic mining region of the Bolivian Altiplano. Sci. Total Environ. 412–413, 170–184.

Goix, S., Resongles, E., Point, D., Oliva, P., Duprey, J., de la Galvez, E., Ugarte, L., Huayta, C., Prunier, J., Zouiten, C., Gardon, J., 2013. Transplantation of epiphytic bioaccumulators (*Tillandsia capillaris*) for high spatial resolution biomonitoring of trace elements and point sources deconvolution in a complex mining/smelting urban context. Atmos. Environ. 80, 330–341.

Guédron, S., Grangeon, S., Jouravel, G., Charlet, L., Sarret, G., 2013. Atmospheric mercury incorporation in soils of an area impacted by a chlor-alkali plant (Grenoble France): Contribution of canopy uptake. Sci. Total Environ. 445–446, 356–364.

Grangeon, S., Guedron, S., Asta, J., Sarret, G., Charlet, L., 2012. Lichen and soil as indicators of an atmospheric mercury contamination in the vicinity of a chlor-alkali plant (Grenoble France). Ecol. Indic. 13, 178–183.

Isaac-Olivé, K., Solís, C., Martínez-Carrillo, M.A., Andrade, E., López, C., Longoria, L.C., Lucho-Constantino, C.A., Beltrán-Hernández, R.I., 2012. *Tillandsia usneoides* L, a biomonitor in the determination of Ce, La and Sm by neutron activation analysis in an industrial corridor in Central Mexico. Appl. Radiat. Isot. 70, 589–594.

Jarup, L., 2003. Hazards of heavy metal contamination. Br. Med. Bull. 68 (1), 167–182.

Langner, P., Mikutta, C., Kretzschmar, R., 2012. Arsenic sequestration by organic sulphur in peat. Nat. Geosci. 5, 66–73.

Li, P., Zheng, G., Chen, X., Pemberton, R., 2012. Potential of monitoring nuclides with the epiphyte *Tillandsia usneoides*: uptake and localization of ^{133}Cs. Ecotoxicol. Environ. Saf. 86, 60–65.

Martin, C.E., Rux, G., Herppich, W.B., 2013. Responses of epidermal cell turgor pressure and photosynthetic activity of leaves of the atmospheric epiphyte *Tillandsia usneoides* (Bromeliaceae) after exposure to high humidity. J. Plant Physiol. 170, 70–73.

Martínez-Carrillo, M.A., Solís, C., Andrade, E., Isaac-Olivé, K., Rocha, M., Murillo, G., Beltrán-Hernández, R.I., Lucho-Constantino, C.A., 2010. PIXE analysis of *Tillandsia usneoides* for air pollution studies at an industrial zone in Central Mexico. Microchem. J. 96, 386–390.

Miller, J.R., Villarroel, L.F., 2011. Bolivia: mining, river contamination, and human health. In: Nriagu, J.O. (Ed.), Encyclopedia of Environmental Health. Elsevier, Burlington, pp. 421–441.

OíNeill, M.S., Osornio-Vargas, A., Buxton, M.A., Sánchez, B.N., Rojas-Bracho, L., Castillo-Castrejon, M., Mordhukovich, I.B., Brown, D.G., Vadillo-Ortega, F., 2013. Air pollution, inflammation and preterm birth in Mexico City: study design and methods. Sci. Total Environ. 448, 79–83.

Papini, A., Tani, G., Di Falco, P., Brighigna, L., 2010. The ultrastructure of the development of *Tillandsia* (Bromeliaceae) trichome. Flora 205, 94–100.

Qian, Z., Dong, G.H., Ren, W.H., Simckes, M., Wang, J., Zelicoff, A., Trevathan, E., 2014. Effect of pet ownership on respiratory responses to air pollution in Chinese children: the Seven Northeastern Cities (SNEC) study. Atmos. Environ. 87, 47–52.

Ravel, B., Newville, M., 2005. ATHENA and ARTEMIS: interactive graphical data analysis using IFEFFIT. J. Synchr. Radiat. 12, 537–541.

Romero-Lankao, P., Qin, H., Borbor-Cordova, M., 2013. Exploration of health risks related to air pollution and temperature in three Latin American cities. Soc. Sci. Med. 83, 110–118.

Ruiz-Castell, M., Paco, P., Barbieri, F.L., Duprey, J.L., Forns, J., Carsin, A.E., Freydier, R., Casiot, C., Sunyer, J., Gardon, J., 2012. Child neurodevelopment in a Bolivian mining city. Environ. Res. 112, 147–154.

Sanchez de la Campa, A.M.S., de la Rosa, J.D., Sanchez-Rodas, D., Oliveira, V., Alastuey, A., Querol, X., Ariza, J.L.G., 2008. Arsenic speciation study of PM2.5 in an urban area near a copper smelter. Atmos. Environ. 42, 6487–6495.

Sarret, G., Pilon Smits, E., Castillo-Michel, H., Isaure, M.P., Zhao, F.J., Tappero, R., 2013. Use of synchrotron-based techniques to elucidate metal uptake and metabolism in plants. Adv. Agron. 119, 1–82.

Schreck, E., Dappe, V., Sarret, G., Sobanska, S., Nowak, D., Nowak, J., Stefaniak, E.A., Magnin, V., Ranieri, V., Dumat, C., 2014. Foliar or root exposures to smelter particles: consequences for lead compartmentalization and speciation in plant leaves. Sci. Total Environ. 476–477, 667–676.

Smodiš, B., Pignata, M.L., Saiki, M., Cortés, E., Bangfa, N., Markert, B., et al., 2004. Validation and application of plants as biomonitors of trace element atmospheric pollution – a coordinated effort in 14 countries. J. Atmos. Chem. 49, 3–13.

Suess, E., Planer-Friedrich, B., 2012. Thioarsenate formation upon dissolution of orpiment and arsenopyrite. Chemosphere 89, 1390–1398.

Szczepaniak, K., Biziuk, M., 2003. Aspects of the biomonitoring studies using mosses and lichens as indicators of metal pollution. Environ. Res. 93, 221–230.

Terán-Mita, T.A., Faz, A., Salvador, F., Arocena, J.M., Acosta, J.A., 2013. High altitude artisanal small-scale gold mines are hot spots for mercury in soils and plants. Environ. Pollut. 173, 103–109.

Thiry, M., Huet-Taillanter, S., Schmitt, J.M., 2002. The industrial waste land of Mortagne-du-Nord (59) – I – assessment, composition of the slags, hydrochemistry, hydrology and estimate of the outfluxes. Bull. Soc. Géol. France 173, 369–381.

Tian, S., Lu, L., Yang, X., Webb, S., Du, Y., Brown, P., 2010. Spatial imaging and speciation of lead in the accumulator plant *Sedum alfredii* by microscopically focused synchrotron X-ray investigation. Environ. Sci. Technol. 44, 5920–5926.

Timmermans, R.M.A., Denier van der Gon, H.A.C., Kuenen, J.J.P., Segers, A.J., Honoré, C., Perrussel, O., Builtjes, P.J.H., Schaap, M., 2013. Quantification of the urban air pollution increment and its dependency on the use of down-scaled and bottom-up city emission inventories. Urban Clim. 6, 44–62.

Uzu, G., Sobanska, S., Sarret, G., Muñoz, M., Dumat, C., 2010. Foliar lead uptake by lettuce exposed to atmospheric fallouts. Environ. Sci. Technol. 44, 1036–1042.

Uzu, G., Schreck, E., Xiong, T., Macouin, M., Lévêque, T., Fayomi, B., Dumat, C., 2014. Urban market gardening in Africa: foliar uptake of metal(loid) s and their bioaccessibility in vegetables; implications in terms of health risks. Water Air Soil Pollut. 225, 1–13.

Van Damme, A., Degryse, F., Smolders, E., Sarret, G., Dewit, J., Swennen, R., Manceau, A., 2010. Zinc speciation in mining and smelter contaminated overbank sediments by EXAFS spectroscopy. Geochim. Cosmochim. Acta 74, 3707–3720.

Vanos, J.K., Hebbern, C., Cakmak, S., 2014. Risk assessment for cardiovascular and respiratory mortality due to air pollution and synoptic meteorology in 10 Canadian cities. Environ. Pollut. 185, 322–332.

Wannaz, E.D., Pignata, M.L., 2006. Calibration of four species of Tillandsia as air pollution biomonitors. J. Atmos. Chem. 53 (3), 185–209.

Wannaz, E.D., Carreras, H.A., Pérez, C.A., Pignata, M.L., 2006. Assessment of heavy metal accumulation in two species of *Tillandsia* in relation to atmospheric emission sources in Argentina. Sci. Total Environ. 361, 267–278.

Wannaz, E.D., Carreras, H.A., Abril, G.A., Pignata, M.L., 2011. Maximum values of Ni^{2+}, Cu^{2+}, Pb^{2+} and Zn^{2+} in the biomonitor *Tillandsia capillaris* (Bromeliaceae): relationship with cell membrane damage. Environ. Exp. Bot. 74, 296–301.

Wannaz, E.D., Carreras, H.A., Rodriguez, J.H., Pignata, M.L., 2012. Use of biomonitors for the identification of heavy metals emission sources. Ecol. Indic. 20, 163–169.

Zhao, F.J., Ma, J.F., Meharg, A.A., McGrath, S.P., 2009. Arsenic uptake and metabolism in plants. New Phytol. 181, 777–794.